



PERFORMANCE EVALUATION OF MIMO-OFDM IMPLEMENTATION ON WIRELESS OPEN-ACCESS RESEARCH PLATFORM (WARP)

Titiek Suryani and Suwadi

Department of Electrical Engineering, Institut Teknologi Sepuluh Nopember (ITS), Surabaya, Indonesia
 E-Mail: titiks@ee.its.ac.id

ABSTRACT

Spatial diversity technique known as multiple-input-multiple-output (MIMO) and multi-carrier modulation technique, one of which is an orthogonal frequency division multiplexing (OFDM) technique, is two candidate techniques that are suitable for use on high-speed data transmission in the future. OFDM technique uses a large number of sub-carriers to overcome the effects of frequency selective fading and using cyclic-prefix to suppress inter-symbol-interference (ISI) caused by multipath propagation. The duration of the cyclic-prefix should be longer than the delay-spread of the multipath channel, so that ISI can be removed completely. The application of MIMO diversity techniques on the OFDM system will improve system performance significantly. By using MIMO techniques, many propagation path will be available. These propagation path are departing from a number of antennas on the transmitter side toward a number of antennas on the receiver side directly. Therefore, if there is a severe distortion signals coming out from one of propagation-path then the system may rely on other signals from other propagation-path. Thus the possibility of errors that may occur can be prevented. Furthermore, to increase the diversity of the fading effect, in this study, we use space-time coding-block-code (STBC) Alamouti. This paper aims to study the combined performance of MIMO-OFDM technique when applied to the Wireless open-Access Research Platform (WARP) module, which is one of the software defined radio (SDR) device. The MIMO-OFDM system performance is analyzed and compared to the MISO-OFDM system, both system use quadrature phase shift keying (QPSK) modulation scheme.

Keywords: MIMO, OFDM, WARP, STBC, Alamouti.

INTRODUCTION

The multiple-input-multiple-output (MIMO) technique has been widely known as spatial diversity or multiplexing techniques which can increase the performance or the capacity of system, especially when working in fading attenuation due to the multipath propagation environments. Even in the high-speed data transmission system, the fading channel characteristics will become very complex, from flat fading channel conditions transformed into the frequency-selective fading channel. To overcome this condition, the high speed data transmission is often used multi-carrier modulation technique known as orthogonal-frequency-division-multiplexing (OFDM).

OFDM technique has become a common technique used for signal transmission through a wireless channel and has been adopted in several wireless standards such as digital audio broadcasting (DAB), digital video broadcasting (DVB-T), IEEE 802.11a [1] for a standard local area network (LAN) and IEEE 802.16a [2] for a standard metropolitan area network (MAN). Even OFDM is a potential candidate for a mobile wireless system.

The OFDM technique divides the wideband spectrum of high-speed data into several narrowband spectrums, so the effect of frequency selective fading can be reduced and the further damage can be localized on just one sub-carrier spectrum. Moreover, due to the orthogonality, many narrowband spectral enable to be overlapped so that the transmission bandwidth becomes more efficient. To overcome the inter-symbol-interference (ISI) distortion, at the beginning of each OFDM symbol.

Wireless open-Access Research Platform (WARP) is developed by Rice University. The platform architecture consists of four key components: custom hardware, platform support packages, open-access repository and research applications; all together providing a reconfigurable wireless testbed for students and faculty. One of the main features of WARP hardware, which makes it distinguishable from other similar boards designed for educational purposes, is its four daughtercard slots that can be used to connect radio boards. These radio boards can be attached to the main board so that up to a 4×4 multiple-input multiple-output (MIMO) system can be built. In this study, the combined technique of MIMO-OFDM is implemented on the WARP module, where the MIMO technique is intended as a diversity technique to get power efficiency by maximizing the spatial diversity by using a space-time block codes (STBC) Alamouti 2×2 [3], [4]. This implementation of MIMO and OFDM system on WARP module requires time synchronization, channel estimation and frequency offset estimation, which is performed by using a preamble consisting of one or more training symbols [5], [6], [7]. The join MIMO-OFDM techniques are compared to the multiple-input-single-output (MISO)-OFDM in the bit-error-rate (BER) system performance.

An overview of OFDM, MIMO and MIMO-OFDM are given in section 2. The implementation of MIMO-OFDM technique on WARP will discussed in section 3 and the discussion and analysis of the performance of MIMO-OFDM system are given in section 4. While, the conclusions are given in section 5.



SYSTEM DESCRIPTION

MIMO Technique

A transmission using multiple antennas technique has long been utilized in wireless communications. The utilization of a number of antennas at the transmitter and receiver of a communication system is the standard method in spatial diversity to anticipate channel fading without increasing the bandwidth of the transmission signal. Generally, the received signal consists of several signals coming from different propagation path. The reliability of the system diversity is obtained, because when the signal from one of propagation path suffer from deep fade, then other signal from the other propagation path that not experiencing deep fade in the same time can be use so that the receiver able to detect and estimate the signal data correctly. This signal can be combined and selected using particular combining techniques. Hence, the system reliability can be improved. Figure-1. [8], an example of a MIMO system, in which the transmitter and the receiver is equipped with a two-element array, respectively. When the MIMO technique is used as a diversity technique, then each transmitting antenna will transmit the same data in different space and time by using space-time-block-code (STBC) coding scheme.

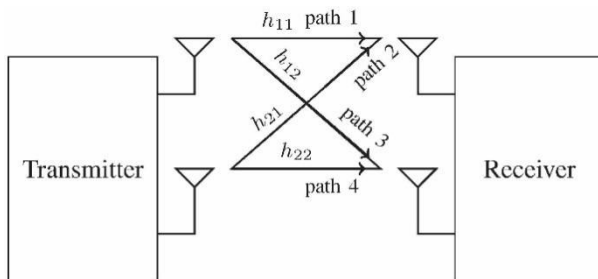


Figure-1. 2×2 MIMO system

The diversity technique scheme that uses two transmitting antennas and two receiver antennas are shown in Figure-1 with channel notations as defined in the figure. The process from transmitter to receiver side consists of three stages:

A. The STBC encoding, the channel parameter for each propagation-path, and the received signal can be explained through Table-1, Table-2, and Table-3, respectively.

Table-1. STBC.

| Time slot | Antenna 1 | Antenna 2 |
|--------------|-----------|-----------|
| time t | s_1 | s_2 |
| time $t + T$ | $-s_2^*$ | s_1^* |

Table-2. Channel notation.

| Tx \ Rx | Antenna 1 | Antenna 2 |
|-----------|-----------|-----------|
| antenna 1 | h_{11} | h_{21} |
| antenna 2 | h_{12} | h_{22} |

Table-3. Received signal.

| Time slot | Antenna 1 | Antenna 2 |
|--------------|-----------|-----------|
| time t | r_1 | r_3 |
| time $t + T$ | r_2 | r_4 |

In the STBC encoding process, the signal sequence will be divided into blocks, with each block consist of two symbols, denote as s_1 and s_2 , this signal will be encoded as $[s_1 - s_2^*]$ and $[s_2 s_1^*]$. These encode signals will be sent through antenna 1 and antenna 2, respectively.

After transmitted through channel, the received signal that arrive at different antenna and time are denoted as:

$$\begin{aligned} r_1 &= s_1 h_{11} + s_2 h_{12} + n_1 \\ r_2 &= -s_2^* h_{11} + s_1^* h_{12} + n_2 \\ r_3 &= s_1 h_{21} + s_2 h_{22} + n_3 \\ r_4 &= -s_2^* h_{21} + s_1^* h_{22} + n_4 \end{aligned} \quad (1)$$

where

r_1 = received signal at antenna 1 and time t .

r_2 = received signal at antenna 1 and time $t + T$.

r_3 = received signal at antenna 2 and time t .

r_4 = received signal at antenna 2 and time $t + T$.

h_{kl} with $k = l = 1, 2$ is a Rayleigh fading channel impulse response, the channel path is from l^{th} antennas at the transmitter to the k^{th} antenna at the receiver.

n_1, n_2 are a thermal noise on the receiver antenna 1 at time t and $t + T$ respectively and n_3, n_4 also a thermal noise on the receiver antenna 2 at time t and $t + T$ respectively.

B. Combining

At the receiver, the combiner provides two combining signal to the input of maximum likelihood detector that expressed as follow:

$$\begin{aligned} \hat{s}_1 &= h_{11}^* r_1 + h_{12}^* r_2^* + h_{21}^* r_3 + h_{22}^* r_4^* \\ \hat{s}_2 &= h_{12}^* r_1 - h_{11}^* r_2^* + h_{22}^* r_3 - h_{21}^* r_4^* \end{aligned} \quad (2)$$

By substituting equation(1) into equation (2), will yields following equation:

$$\begin{aligned} \hat{s}_1 &= (\alpha_{11}^2 + \alpha_{12}^2 + \alpha_{21}^2 + \alpha_{22}^2) s_1 + h_{11}^* n_1 \\ &\quad + h_{12}^* n_2^* + h_{21}^* n_3 + h_{22}^* n_4^* \\ \hat{s}_2 &= (\alpha_{11}^2 + \alpha_{12}^2 + \alpha_{21}^2 + \alpha_{22}^2) s_2 - h_{11}^* n_2^* \\ &\quad + h_{12}^* n_1 - h_{21}^* n_4^* + h_{22}^* n_3 \end{aligned} \quad (3)$$

The coefficient value of the desired symbol will be further away from the value of unwanted symbol.



C. Maximum likelihood detector process

In the detection stage, the received signal will be estimated based on euclidean distance between received signal and reference signal.

OFDM Technique

In the OFDM transmitter, bit sequence is converted into symbol sequence correspond to the selected modulation scheme, such as QPSK ($M = 4$), M -ary QAM, etc. The symbol duration is defined and denoted as $T_s = (\log_2 M)T_b$, with T_b is the duration of the data bit. The serial symbols sequence is then converted into parallel symbols sequence. The Number of symbol in parallel corresponds to the number of available sub-carriers. If the number of sub-carrier = N_{sc} , then the OFDM symbolperiod is $T_{OFDM} = N_{sc}T_s$. These symbols will modulate the sub-carriers signal respectively. The distance between the adjacent sub-carrier is $\Delta f = 1/T_{OFDM}$. The modulated sub-carrier signal is then multiplexed into one OFDM symbol. This process is called as multi-carrier modulation and can be realized using an inverse fast Fourier transform (IFFT) algorithm. At the receiver, the demodulation process is performed by using FFT algorithm. So that the block diagram of OFDM transmitter and receiver can be illustrated in the Figure-2 and Figure-3.

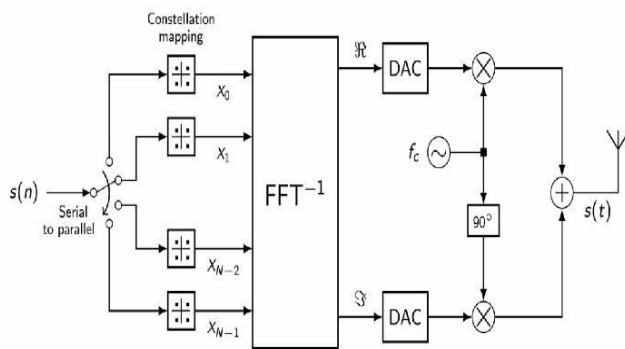


Figure-2. The OFDM transmitter system.

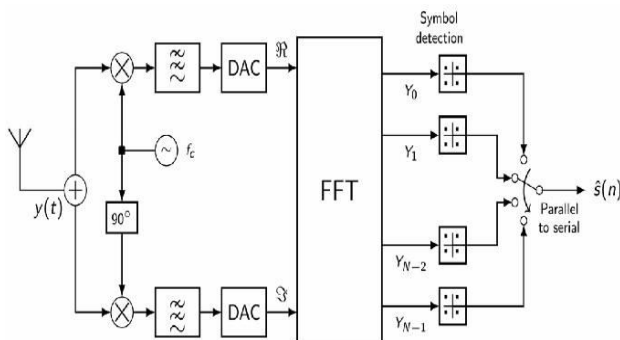


Figure-3. The OFDM receiver system.

The mapping blocks in Figure-2 map the data bits into data symbols according to the constellation of the modulation scheme, for example if we use QPSK, the bit stream is divided into blocks consisting of $m = \log_2 M =$

$\log_2 4 = 2$ bits, so there are four possible combinations, namely: 00, 01, 10 and 11 which will be mapped to the QPSK symbol as shown in Table-4.

Table-4. QPSK mapping.

| | 0 | 1 |
|---|---------------------|---------------------|
| 0 | $-0.7071 - i0.7071$ | $-0.7071 + i0.7071$ |
| 1 | $0.7071 - i0.7071$ | $0.7071 + i0.7071$ |

In the OFDM technique, not all the data sub-carriers are allocated for data symbol but also allocated for pilot symbols that are required for channel estimation purposes at receiver side [9]. There are several options of pilot structures [10]; one of the structures is comb-type as shown in Figure-4. In this type, the pilot symbols are arranged periodically in several sub-carriers, then by interpolation in the frequency domain, the channel frequency response will be estimated. In addition, the pilot symbols in this type should also be placed on a coherent bandwidth. The coherence bandwidth is inversely proportional to the maximum delay spread, which is denoted by σ_{max} , so we get the equation (4).

$$S_f \leq \frac{1}{\sigma_{max}} \quad (4)$$

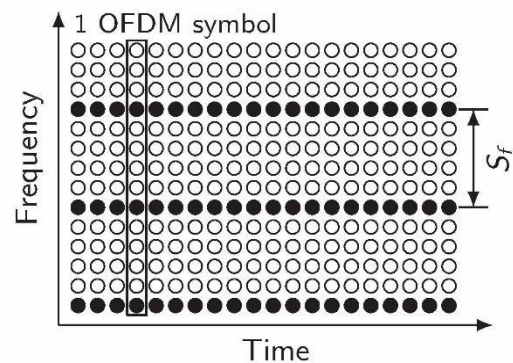


Figure-4. Comb-type pilot structure.

MIMO-OFDM Technique

In the MIMO-OFDM system, the parallel symbols before delivered to the IFFT input will encode first using space-time-block-code (STBC) coding scheme. The STBC coder will produce two parallel symbol as described as follow, suppose the 1 block of two parallel symbols is expressed as: $[s_1 s_2]$, then, this block of two parallel symbols is encode to become two block as follow: $[s_1 s_2^*]$ and $[s_2 s_1^*]$, the first block will be sent to the branch to the antenna 1 and the second will be sent to the branch to the antenna 2 for further processing. The MIMO-OFDM system is shown in Figure-5 (a) for transmitter and Figure-5 (b) for receiver.

MIMO-OFDM IMPLEMENTATION ON WARP

The block diagram implementation of MIMO-OFDM technique on the WARP module is shown in



Figure-5 (a) and Figure-5 (b). The transmit data bit is mapped into values according to the type of modulation scheme (in this research is QPSK), so the bit sequences consists of bit 1 and 0 is changed into sequences consists of four complex values $\pm 0.7071 \pm i0.7071$, where $i = \sqrt{-1}$. In the baseband complex form this conversion is shown in Table-4. The serial-to-parallel block convert the data sequences into a matrix with a size $N_{data} \times N_{sym}$, where N_{data} is a number of data in a single OFDM symbol and N_{sym} is a number of OFDM symbol that will be transmitted. In WARP, we use 64 sub-carrier that are allocated as follow: 48 sub-carriers are assigned for data symbols (i.e. sub-carrier number : 2-7, 9-21, 23-27, 39-43, 45-57, 59-64) and 4 sub-carriers (i.e. sub-carrier number: 8, 22, 44, 58) for pilots and the remaining sub-carriers left empty for Doppler estimation purposes. Before further processed in IFFT block, the data symbols and pilots will be encoded by STBC encoder using Alamouti coding scheme. The encoding process can be explained as follow. Suppose that the IFFT input is expressed in matrix form as: $[s_1 s_2 s_3 s_4 \dots s_{sym-1} s_{sym}]$,

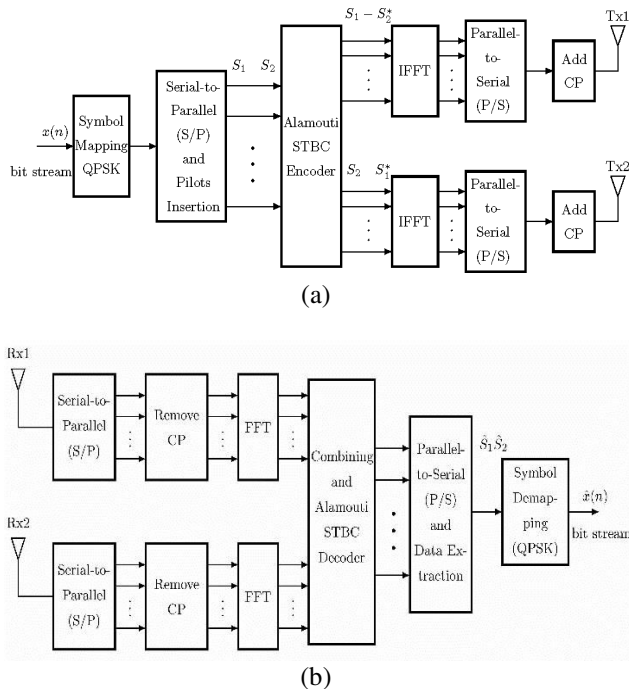


Figure-5(a). MIMO-OFDM transmitter system and **(b).** MIMO-OFDM receiver system.

where s_i is a vector which contains data symbols and pilots to be converted as i^{th} OFDM symbol. The STBC encoder will encode this matrix elements and provides two different matrix with elements as follow: $[s_1 - s_2^* s_3 - s_4^* \dots s_{sym-1} - s_{sym}^*]$ and $[s_2 s_1^* s_4 s_3^* \dots s_{sym} s_{sym-1}^*]$. Output of the IFFT blocks are converted in serial form by parallel-to-serial converter and cyclic prefix is added to each OFDM symbol.

For synchronization and channel estimation purposes, some preambles are added to the data frame.

There are two kind of preambles, i.e. Long Training Symbol (LTS) and Short Training Symbol (STS). These preamble shown in Figure-6. After that, the signal is interpolated to increase the sampling rate and then signal will be carried by higher frequency carrier signal [11] and will be radiated by antenna-1 and antenna-2, simultaneously.

The interpolation process is divided into two steps: up-sampling and low-pass-filtering (LPF) [13]. After this process, signal will be normalized and will be sent to the buffer transmitter through Ethernet. This transmission process will start after the synchronization packet is sent to the transmitter node. Meanwhile in the receiver: the received signal will be decimated. The decimation process is divided into two steps : low-pass filtering and down-sampling that is the opposite of up-sampling in transmitter process [14].

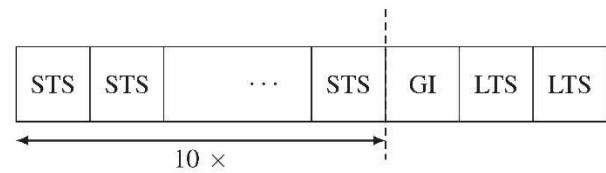


Figure-6. Preamble structure [12].

After the decimation process, the received preamble will be cross-correlated with LTS reference using following equation [15],

$$C(n) = \sum_{l=0}^M \sum_{k=0}^N r(lN + k + n) s^*(lN + k) \quad (6)$$

Where r is the total received preamble, s is one unit LTS, N is OFDM data length and M is number of cross correlated LTS. The cross-correlation process is performed for synchronisation process so that the start of each frame can be determined [16]. An example of cross-correlation result is shown in Figure-7 [7].

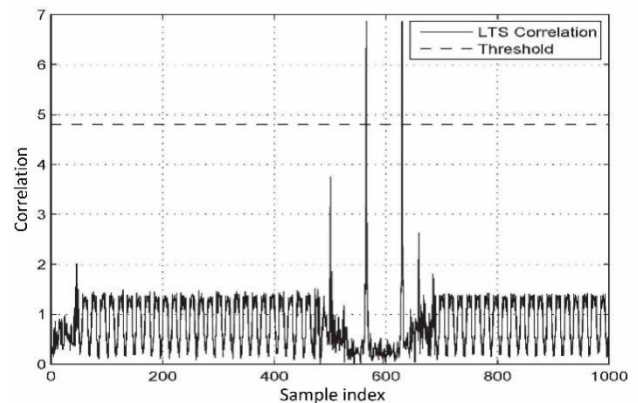


Figure-7. LTS Correlation

From the two peak values in this , the LTS location will be determined and the beginning of the first OFDM frame is known, the next step is removing the cyclic prefix part and than FFT process is applied using 64-point. Following FFT process is Doppler frequency



estimation and correction. Furthermore, the magnitude channel response and the phase channel response are estimated that are required in combining and decoder STBC process. Finally, the data symbols are converted back to the bit sequence by de-mapping QPSK constellation process.

Frame design for communication using WARP is based on parameter in [17], for example, number of buffer in WARP is limited to 214 or 16,384 sample and sampling rate of the system is 40 MHz. This frame design process is to meet the signal structure with the WARP specification. For each frame, some field should be provided for delay margin. This delay comes from propagation delay and data acquisition in WARP, delay value is allocated in 2,944 sample and is located in the end of frame using 0's, so this delay is called as zero padding. The frame design for communication is shown in Figure-8.

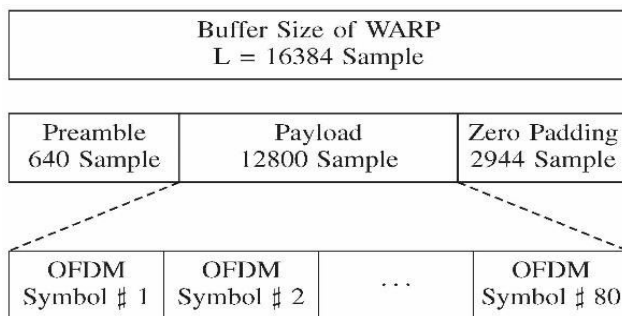


Figure-8. Frame structure for communication.

For addition, all of OFDM symbol are not only containing some data but also cyclic-prefix, pilot or training symbol and virtual sub-carrier.

DISCUSSION AND RESULT

The system parameter specification of the implementation of MIMO-OFDM technique on WARP module are given in Table-5.

Table-5. System parameter specification.

| Parameter | Specification |
|--|------------------------|
| Bit rate | 24 Mbps |
| QPSK symbol rate per carrier (baud rate) | 12 MBd |
| Number of subcarrier | 64 (48 data + 4 pilot) |
| OFDM symbol rate | 250 kDd |
| Cyclic prefix ratio | 25% |
| Number of data bit | 107,520 bit |
| Setting gain in WARP: | |
| Tx baseband | 2 |
| Tx RF | 0-60 |
| Rx baseband | 2 |
| Rx RF | 2 |
| MIMO size | 2 × 2 |
| Diversity Coding System | STBC Alamouti |

There are many scatter plot patterns of data symbols after travelling through channel and after processing in Alamouti decoding, as shown in Figure-9.

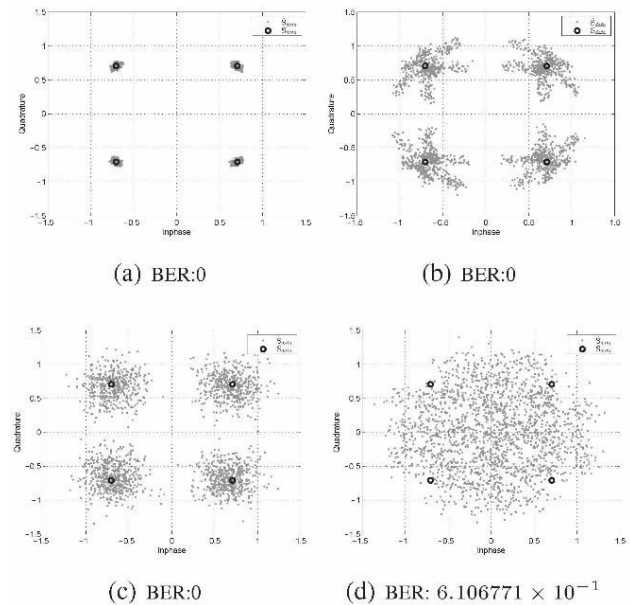


Figure-9. Scatter plot after decoding Alamouti

- The difference in the scatter pattern is caused by:
- Fading attenuation.
 - Noise interference.
 - Interference from existing WiFi equipment operates on the 2.4 GHz band.
 - Carrier frequency offset (CFO) and phase offset residue.
 - Capability of channel estimation and CFO estimation of the receiver.
 - Accurate LTS cross-correlation calculation.

Among the scatter plot patterns, Figure-9. (a) is the best receiver output estimation and detection results. This pattern is frequently occur when the receiver power compared to the noise power spectral density is relative small, no moving objects in the surrounding environment, and no interference coming from WiFi nearby. In this condition, the channel estimation results is relatively accurate. Furthermore, the cross-correlation calculation for synchronization purpose also accurate.

The scatter plot pattern as shown in part (b) Figure-9. may also occur. According to [15], this pattern appears when the carrier frequency offset (CFO) and phase offset not well estimated. Although, the receiver has been equipped with CFO and phase offset correction to overcome the Doppler effect and the impact of transmitter and receiver clocks independency, but these impairment are not completely eliminated. If the CFO is too large, i.e.



more than 10 % of the distance between adjacent sub-carriers, the estimation become inaccurate and leave a residual CFO. This condition becomes more severe if the power noise or fading attenuation is very large, so the scattering pattern will spread and bit error will occur. This condition is possible if there are moving objects around the transmitter and the receiver.

The scatter plot pattern in Figure-9. (c) may occur when the Doppler and the fading attenuation is small, but the signal experienced large noise power. The small CFO due to the Doppler effect can be completely removed by the receiver. If the noise power is not too large, then detection will be able to estimate all the transmitted data bits correctly (bit error rate (BER) = 0). On the other hand, if the noise power is very large then there will be the possibility of the signal is located in the wrong decision-region, hence $BER \neq 0$.

There are several possibilities that causes scatter plot pattern as shown in Figure-9. (d). Large noise power or large fading attenuation, both have high impact on the channel estimation and correction results. The LTS cross-correlation calculation not accurate because the training symbol suffering from interference or severe distortion, this condition will make system loses symbol synchronization, hence the channel estimation result will be not accurate. In general, the scatter plot pattern like Figure-9. (d) often occurs if the signals are transmitted with relative small power transmit or if the distance between transmitter and receiver relatively large and the interference from nearby WiFi is high. Furthermore, this condition will result in high bit error rate.

It should be noted that the effect of fading attenuation is not appear on the scatter plot, this is because the data signal was normalized first before plotting process.

The BER system performance in indoor and outdoor condition for a distance of 4 meters from measurement is given in Figure-10. This figure comparing the BER system performance between the MIMO-OFDM and MISO-OFDM system, from the curve can be seen that there is a significant improvement of the BER system performance when using MIMO-OFDM technique in both indoor and outdoor environments. The difference between indoor and outdoor performance is because of the number of moving objects in outdoor is more than the indoor, beside that the interferences from number of active WiFi are stronger.

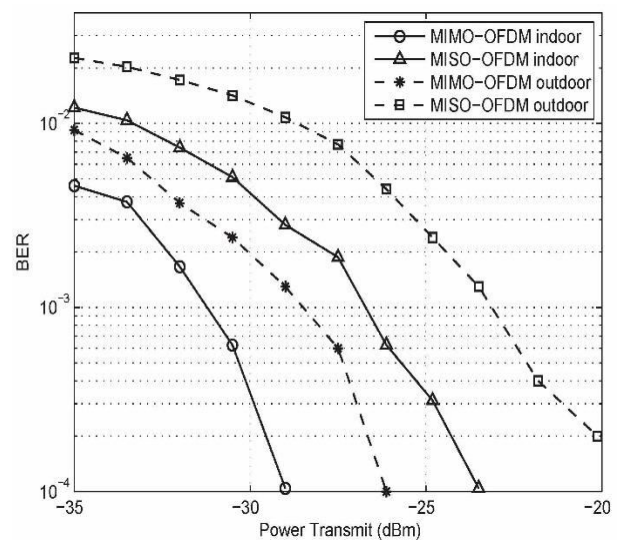


Figure-10. BER MIMO-OFDM system performance.

The example of moving object is people walking around the measurement location. The presence of moving objects around the test device will generate the CFO distortion due to the Doppler effect. In addition, the noise power interference in outdoor is greater than indoor because the outdoor temperature is higher than indoor.

CONCLUSIONS

From BER system performance curve it is shown that the MIMO-OFDM can be implemented on WARP module. The significant BER performance improvement is obtained when using MIMO-OFDM system than MISO-OFDM system. The difference between indoor and outdoor performance for both systems MIMO-OFDM and MISO-OFDM because the outdoor impairment such as: CFO, noise signal power and WiFi interference is greater than indoor. The number of moving objects and the temperature at outdoor are greater than indoor, both caused CFO and noise power increases, respectively. In addition, the location of some WiFi access point devices are also closer to the outdoor device location than indoor, so that the outdoor interference became greater than indoor.

ACKNOWLEDGEMENTS

The reported work is part of research program funded by the Excellence Research Grant 'Penelitian Unggulan Perguruan Tinggi (PUPT)' 2015-2016 from the Ministry of Research, Technology and Higher Education of the Republic of Indonesia.

REFERENCES

- [1] Part 11. 1999. Wireless LAN Medium Access Control (MAC) and Physical Layer (PHY) Specifications: High-Speed Physical Layer in the 5 GHz Band, IEEE Standard 802.11a-1999.



- [2] Local and Metropolitan Area Networks-Part 16, Air Interface for Fixed Broadband Wireless Access Systems}, IEEE Standard IEEE 802.16a.
- [3] S. Alamouti. 1998. A simple transmit diversity technique for wireless communications. IEEE J. Select. Areas Commun. 16: 1451-1458.
- [4] V. Tarokh, H. Jafarkhani and A. R. Calderbank. 1999. Space-time block codes from orthogonal designs. IEEE Trans. Inform. Theory. 45: 1456-1467.
- [5] Suwadi, T. Suryani and I. Anisah. 2016. Performance analysis of cooperative communication systems using wireless open access research platform for indoor and outdoor environment. Journal of Theoretical and Applied Information Technology. 83(3): 474-481.
- [6] R. S. Darwis, Suwadi, Wirawan, Endroyono, T. Suryani, P. H. Mukti. 2014. Implementation and performance analysis of Alamouti algorithm for MIMO 2x2 using Wireless Open Access Research Platform (WARP). Proceeding of International Conference on Information Technology, Computer, And Electrical Engineering (ICITACEE). pp.436-440.
- [7] T. Suryani, Suwadi, Hasan and S. W. Yoga. 2015. Implementation and performance evaluation of orthogonal frequency division multiplexing (OFDM) using WARP. International Seminar on Intelligent Technology and Its Applications (ISITIA). pp. 451-456.
- [8] N. Costa and S. Haykin. 2010. Multiple-input multiple-output channel models: Theory and practice, John Wiley and Son, Inc.
- [9] V. S. Abhayawardhana and I.J. Wassell. 2002. Common Phase Error Correction with Feedback for OFDM in Wireless Communication. IEEE Global Telecommunications Conference.
- [10] Yong Soo, Cho, Jaekwon Kim, Won Young Yang and Chung G. Kang. 2010. MIMO-OFDM wireless communications with MATLAB, John Wiley & Sons.
- [11] Vercimak, Luke., and Karl Weyeneth., Software Defined Radio Bradley University.
- [12] Mody, Apurva N. and Gordon L. Stuber. 2001. Synchronization for MIMO OFDM systems. Global Telecommunications Conference, 2001. GLOBECOM'01. IEEE. Vol. 1. IEEE.
- [13] Cho, Yong Soo., Jaekwon Kim., Won Young Yang., Chung-Gu Kang. 2010. MIMO-OFDM Wireless Communications with MATLAB}, John Wiley and Sons (Asia) Pte Ltd, Singapore.
- [14] Hayes, Monson H. 1999. Schaum's Outline of Theory and Problems of Digital Signal Processing, USA.
- [15] Hwang, Taewon., Chenyang Yang., Gang Wu., Shaoqian Li., Geoffrey Ye Li. 2009. OFDM and Its Wireless Applications: A Survey. IEEE Transactions on Vehicular Technology. 58(4).
- [16] WARP Project-Wireless Open Access Research Platform, WARP Radio Board Overview, URL: <http://warpproject.org/trac/wiki/HardwareUsersGuides/RadioBoard>.
- [17] L. Brotje, S. Vogeler, K-D Kammeyer, R. Ruckriem and S. Fechtel. 2003. On Carrier Frequency Offsets in Alamouti-coded OFDM systems similar to IEEE 802.11., matrix. 4(65): 7.